Dynamics of Boolean Networks: An Exact Solution

Alexander Mozeika and David Saad

The Non-linearity and Complexity Research Group, Aston University, Birmingham B4 7ET, United Kingdom

(Received 8 January 2011; published 24 May 2011)

The dynamics of Boolean networks (BN) with quenched disorder and thermal noise is studied via the generating functional method. A general formulation, suitable for BN with any distribution of Boolean functions, is developed. It provides exact solutions and insight into the evolution of order parameters and properties of the stationary states, which are inaccessible via existing methodology. We identify cases where the commonly used annealed approximation is valid and others where it breaks down. Broader links between BN and general Boolean formulas are highlighted.

DOI: 10.1103/PhysRevLett.106.214101 PACS numbers: 05.45.−a, 87.16.Yc

In his seminal work [1] Kauffman introduced a simple dynamical model of gene-regulatory networks. The state of each gene was modeled by an on/off variable, interacting with other genes via a coupling Boolean function which determines the state of a gene at the next time step. There are N such genes (sites) in the network and each one is influenced by exactly k other genes from the same network. In Kauffman's approach, the networks are constructed in a random manner by choosing Boolean functions from the set of all 2^{2^k} functions of k inputs and by connecting the inputs of each function to randomly selected genes from the set $1, \ldots, N$; Boolean functions and connections are fixed for all subsequent time steps (quenched variables). The evolution of such a system is deterministic, and since the number of states is finite (2^N) the system is driven to a periodic-orbit attractor.

It was argued [1] that, despite its simplicity, this model, also known as random Boolean network (RBN) or Kauffman net, is of relevance to the understanding of biological systems and has been studied primarily for this reason [2]. RBN belongs to a larger class of Boolean networks, the N-k model of N-variable dynamical systems with a discrete state space and k-variable interactions, that exhibits a rich dynamical behavior [3,4]. The N-k model is very versatile and has found its use in the modeling of genetic networks [5], neural networks [6], social networks [7], and in many other branches of science [3,4].

For over two decades the annealed approximation [8] has proved to be a valuable tool in the analysis of large scale Boolean networks ($N \to \infty$) as it allows one to predict the time evolution of network activity (proportion of on/off states) and Hamming distance (the difference between the states of two networks of identical topology) order parameters. The latter was used [8] to predict a phase transition at $k = 2$ in RBN. The main assumption in this method is to ignore the fact that both Boolean function types and random connections in a Boolean network are quenched variables; it enables one to resample them at each time step and ignore potential correlations among input variables, which simplifies the analytical treatment significantly. It was shown [9,10] that the annealed approximation indeed gives a correct result for the Hamming distance order parameter in RBN, but the broad validity of the annealed approximation to general networks of this type has remained an open problem [11]. Remarkably, the annealed approximation provides accurate activity and Hamming distance results for many other Boolean models with quenched disorder but cannot compute correlation functions, used in studying memory effects, due to the repeated resampling at different time steps that makes the various quenched systems indistinguishable. Furthermore, there are models [12] that have very strong memory effects in specific regimes, where the annealed approximation is no longer valid.

In this Letter, we study the dynamics of the N-k model with quenched disorder and thermal noise using the generating functional analysis, an established method for studying physical systems of this type [13]; the analysis is general and covers a large class of recurrent Boolean networks and related models. We show that results for the Hamming distance and network activity obtained via the quenched and annealed approaches, for the N-k model, are identical. In addition, stationary solutions of the Hamming distance and two-time autocorrelation function (inaccessible via the annealed approximation) coincide, giving insight into the uniform mapping of states within the basin of attraction onto the stationary states. In the presence of noise, we show that above some noise level the system is always ergodic and explore the possibility of a spin-glass phase [14] below this level. Finally, we show that our theory can be used to study the dynamics of models with strong memory effects.

The model considered is an N-variable recurrent Boolean network with the parallel update rule

$$S_i(t+1) = \alpha_i(S_{i_1}(t), \ldots, S_{i_k}(t)), \tag{1}$$

where $S_i(t) \in \{-1, 1\}$ and $\alpha_i : \{-1, 1\}^k \to \{-1, 1\}$ is a Boolean function of exactly k inputs. The thermal noise flips the output of a function with probability p [15].

The function at site i and time step $t+1$ operates in a stochastic manner according to the microscopic law

$$P_{\alpha_i}(S_i(t+1)|S_{i_1}(t),\ldots,S_{i_k}(t)) \propto e^{\beta S_i(t+1)\alpha_i(S_{i_1}(t),\ldots,S_{i_k}(t))}, \quad (2)$$

where the inverse temperature $\beta = 1/T$ relates to the noise parameter p via $\tanh\beta = 1-2p$. The function output $S_i(t+1)$ is completely random or deterministic when $\beta \to 0$ or ∞, respectively. Given the state of the network $\boldsymbol{S}(t) \in \{-1,1\}^N$ at time t the functions at time $t+1$ are independent of each other. This suggests that the probability of the microscopic path $\boldsymbol{S}(0) \to \cdots \to \boldsymbol{S}(t_{\max})$ is a product of (2) over sites and time steps. The joint probability of microscopic states in two systems of identical topology but subject to different thermal noise or initial conditions is

$$P[\{\boldsymbol{S}(t)\};\{\hat{\boldsymbol{S}}(t)\}] = P(\boldsymbol{S}(0),\hat{\boldsymbol{S}}(0)) \times \prod_{t=0}^{t_{\max}-1} P(\boldsymbol{S}(t+1)|\boldsymbol{S}(t))P(\hat{\boldsymbol{S}}(t+1)|\hat{\boldsymbol{S}}(t)), \quad (3)$$

where $P(\boldsymbol{S}(t+1)|\boldsymbol{S}(t)) = \prod_{i=1}^N P_{\alpha_i}(S_i(t+1)|S_{i_1}(t),\ldots,S_{i_k}(t))$.

The quenched disorder in our model arises from the random sampling of connections and Boolean functions generated by selecting the ith function and sampling exactly k indices, $\{i_1,\ldots,i_k\}$, uniformly from the set of all possible indices. Boolean functions $\{\alpha_i\}$ are sampled randomly and independently from a given distribution of k-ary Boolean functions. To analyze the typical properties of the system via the generating functional method, one defines

$$\Gamma[\boldsymbol{\psi};\hat{\boldsymbol{\psi}}] = \langle e^{-i\sum_{t,i}\{\psi_i(t)S_i(t)+\hat{\psi}_i(t)\hat{S}_i(t)\}}\rangle, \quad (4)$$

where $\langle\cdots\rangle$ denotes the average over the joint probability (3). The generating function (4) is used to compute moments of (3) by taking partial derivatives with respect to the generating fields $\{\psi_i(t), \hat{\psi}_j(s)\}$, e.g., $\langle S_i(t)\hat{S}_j(s)\rangle = -\lim_{\boldsymbol{\psi},\hat{\boldsymbol{\psi}}\to 0}\frac{\partial^2}{\partial\psi_i(t)\partial\hat{\psi}_j(s)}\Gamma[\boldsymbol{\psi};\hat{\boldsymbol{\psi}}]$. We assume that the system becomes self-averaging for $N\to\infty$ [13] and compute $\overline{\Gamma[\boldsymbol{\psi};\hat{\boldsymbol{\psi}}]}$, where $\overline{\cdots}$ is the disorder average over the random connection between nodes; this gives rise to the macroscopic observables

$$m(t) = \frac{1}{N}\sum_{i=1}^N \overline{\langle S_i(t)\rangle}, \qquad C(t,s) = \frac{1}{N}\sum_{i=1}^N \overline{\langle S_i(t)S_i(s)\rangle}$$
$$C_{12}(t) = \frac{1}{N}\sum_{i=1}^N \overline{\langle S_i(t)\hat{S}_i(t)\rangle}, \quad (5)$$

where $m(t)$ is the network activity (or magnetization [16]), $C(t,s)$ is the correlation between two states of the same network, and $C_{12}(t)$ the overlap between two copies of the same network (related to the Hamming distance $d(t)$ via $d(t) = \frac{1}{2}[1-C_{12}(t)]$).

Averaging (4) over the disorder [17] leads to the saddle point integral $\overline{\Gamma[\cdots]} = \int\{dPd\hat{P}\}e^{N\Psi[P,\hat{P}]}$, where

$$\Psi = i\sum_{\boldsymbol{S},\hat{\boldsymbol{S}}}\hat{P}(\boldsymbol{S},\hat{\boldsymbol{S}})\mathrm{P}(\boldsymbol{S},\hat{\boldsymbol{S}}) + \log\sum_{\boldsymbol{S},\hat{\boldsymbol{S}}}P(\boldsymbol{S},\hat{\boldsymbol{S}})e^{-i\hat{P}(\boldsymbol{S},\hat{\boldsymbol{S}})}. \quad (6)$$

For $N\to\infty$ the averaged generating functional is dominated by the extremum of Ψ. Functional variation with respect to the order parameters $P(\boldsymbol{S},\hat{\boldsymbol{S}})$ and $\hat{P}(\boldsymbol{S},\hat{\boldsymbol{S}})$ provides the saddle point equation

$$P(\boldsymbol{S},\hat{\boldsymbol{S}}) = P(S(0),\hat{S}(0))\sum_{\{\boldsymbol{S}_j,\hat{\boldsymbol{S}}_j\}}\prod_{j=1}^k[P(\boldsymbol{S}_j,\hat{\boldsymbol{S}}_j)] \times\Big\langle\prod_{t=0}^{t_{\max}-1}P_\alpha(S(t+1)|S_1(t),\ldots,S_k(t)) \times P_\alpha(\hat{S}(t+1)|\hat{S}_1(t),\ldots,\hat{S}_k(t))\Big\rangle_\alpha. \quad (7)$$

The physical meaning of (7) relates to the average joint probability of single-spin trajectories $\boldsymbol{S}$ and $\hat{\boldsymbol{S}}$ in the two systems $P(\boldsymbol{S},\hat{\boldsymbol{S}}) = \lim_{N\to\infty}\frac{1}{N}\sum_{i=1}^N\overline{\langle\delta[\boldsymbol{S};\boldsymbol{S}_i]\delta[\hat{\boldsymbol{S}};\hat{\boldsymbol{S}}_i]\rangle}$, while the conjugate order parameter $\hat{P}(\boldsymbol{S},\hat{\boldsymbol{S}})$ is a constant. Equation (7) is used to compute the macroscopic observables (5), for both noisy ($\beta<\infty$) and noiseless ($\beta\to\infty$) cases, which evolve in time as follows below

$$m(t+1) = f_\alpha(m(t)) = \tanh(\beta)\sum_S\prod_{j=1}^k\Big[\frac{1+S_jm(t)}{2}\Big]\langle\alpha(S)\rangle_\alpha, \quad (8)$$

$$C(t+1,s+1) = F_\alpha(m(t),m(s),C(t,s)) = \tanh^2(\beta)\sum_{S,\hat{S}}\prod_{j=1}^k\Big[\frac{1+S_jm(t)+\hat{S}_jm(s)+S_j\hat{S}_jC(t,s)}{4}\Big] \times\langle\alpha(S)\alpha(\hat{S})\rangle_\alpha, \quad (9)$$

$$C_{12}(t+1) = F_\alpha(m(t),\hat{m}(t),C_{12}(t)), \quad (10)$$

where $S=(S_1,\ldots,S_k)$ and the magnetization $\hat{m}(t)$ is computed by (8).

Results for the order parameters (8)–(10), in combination with (7), suggest that the evolution of all many-time single-site correlation functions is driven by the magnetization $m(t)$. A similar scenario was observed in recurrent asymmetric neural networks [18], defined on comparable topology due to similarity in the equations for $m(t)$ and $C(t,s)$. This is not surprising since the asymmetric neural network is a special case of the N-k model when only linear threshold Boolean functions are used. Furthermore, for the stationary solution $m = f_\alpha(m)$ [$m = \lim_{t\to\infty}m(t)$], the solutions of $q = F_\alpha(m,m,q)$ [here $q = \lim_{t\to\infty}\lim_{\tau\to\infty}C(t+\tau,\tau)$ is the

Edwards-Anderson order parameter, used in disordered systems [14] to detect the spin-glass phase where $m = 0$ and $q \neq 0$] and $C_{12} = F_\alpha(m, m, C_{12})$ are identical. This identity suggests that $q = C_{12}$ and thus a single average Hamming distance $\frac{1}{2}(1 - q)$ on the attractor [19]; all points in the basin of attraction uniformly cover the stationary states.

Annealed model.—Here connectivities and Boolean functions change at each time step (1), providing identical results for m and C_{12} to those of (8) and (10) [11]. However, the annealed correlation function $C(t, s) = m(t)m(s)$, where $t > s$, is the solution of (9) only when networks are constructed from a single function type.

The annealed result [8] for RBN can be easily recovered from Eqs. (8)–(10) using the property $\langle \alpha(S) \rangle_\alpha = 0$ for all $S \in \{-1, 1\}^k$ and $\langle \alpha(S)\alpha(\hat{S}) \rangle_\alpha = 0 \ \forall S \neq \hat{S}$, where the α average is taken over all Boolean functions with equal weight. In this case, the magnetization $m(t) = 0$ for all $t > 0$ and $q = \tanh^2(\beta)(\frac{1+q}{2})^k$, corresponding to the stationary solution of (9), has one stable solution $q \neq 0$ for all finite β and k. For $\beta \to \infty$ (no noise), a transition is observed from one stable solution $q = 1$ for $k \leq 2$ to two solutions $q = 1$ (unstable) and $q \neq 0$ (stable) for $k > 2$ [8].

Ferromagnetic phase.—The unordered paramagnetic phase with $m = 0$ is a fixed point of (8) only when $\sum_S \langle \alpha(S) \rangle_\alpha = 0$. This is a stable and unique solution of (8) when

$$\tanh\beta < \left\{ 2^{k-1}/k \binom{k-1}{(k-1)/2}; 2^{k-2}/(k-1) \binom{k-2}{(k-2)/2} \right\} \equiv b(k)$$

for k odd and even, respectively. To prove this [17] we compare $f_\alpha(m)$ with $f_\chi(m)$, where χ is any balanced Boolean function (with an equal number of ± 1 in the output) from the set [20] $\chi(S) = \mathrm{sgn}[\sum_{j=1}^k S_j] + \delta[0; \sum_{j=1}^k S_j]\gamma(S)$. Thus, the ordered (ferromagnetic) phase $m \neq 0$ is a fixed point of (8) (if at all) only for β and k values which satisfy $\tanh\beta > b(k)$. Similar results, for odd k only, have been conjectured using the annealed approximation and multiplexing techniques [21].

Spin-glass phase.—For $\lim_{t\to\infty} m(t) = m$, $q = 0$ is a fixed point of (9) if and only if $\langle \{\sum_S \alpha(S)\}^2 \rangle_\alpha = 0$, which occurs only for balanced Boolean functions. By a similar argument to the one used in the previous paragraph, we show [17] that for $m = 0$ the point $q = 0$ is a unique stable solution of (9) when $\tanh^2\beta < b(k)$. The α averages in Eqs. (8) and (9) can be computed for a uniform distribution over all balanced Boolean functions to obtain $m(t) = 0$ for all $t > 0$, which implies $q = \tanh^2(\beta)[(\frac{1+q}{2})^k(1 + \frac{1}{2^k-1}) - \frac{1}{2^k-1}]$. The latter has only one $q = 0$ trivial solution for any finite β and develops a second $q = 1$ solution only for $\beta \to \infty$. Thus, the glassy case of $m = 0$, $q \neq 0$ and finite β occurs only (if at all) when $\tanh^2\beta > b(k)$ and for nonuniform distributions over the balanced Boolean functions.

The upper bound $b(k)$ computed here for k odd is identical to the one computed for noisy Boolean formulas [22]. This is since each site i at time t in our model can be associated with the output $S_i(t)$ of a k-ary Boolean formula of depth t which computes a function of the associated initial states [a subset of $\{S_i(0)\}$] [9]. In the presence of noise, a formula of considerable depth (large t) loses all input information for $\tanh\beta < b(k)$ and odd k [22]. This suggests that the upper bound $b(k)$, for odd k, is more general and is valid for transitions at all m values identifying the point where stationary states depend on the initial states and ergodicity breaks. For k even, such general threshold is not yet known.

Memory effects.—In model (1) the state of site i at time t depends on its states at previous times only indirectly. In the limit of $N \to \infty$ these dependencies become weak and Eq. (7) factorizes; this enables one to calculate the observables of interest (8)–(10). However, in a broad family of models [23,24] the state of a site i at a time $t + 1$ depends directly on its state at time t. An exemplar model with strong memory effects used to construct a model of cell-cycle regulatory network ($N = 11$) of budding yeast [25] is of the form

$$S_i(t + 1) = \mathrm{sgn}[h_i(t) - 2h] + S_i(t)\delta[h_i(t); 2h], \quad (11)$$

where $h_i(t) = \sum_{j=1}^k \xi_{i_j}(1 + S_{i_j}(t))$ and $\xi_{i_j} \in \{-1, 1\}$. Mean-field theory ($N \to \infty$) was derived [12] using the annealed approximation in a variant of this model, where the interactions $\{\xi_j\}$ were randomly distributed $P(\xi_j = \pm 1) = 1/2$. Significant discrepancies between the theory and simulation results have been pointed out [12] for integer h values [in this case it is possible that $2h = h_i(t)$], which were attributed to the presence of strong memory effects. Refinements of the annealed approximation method improved the results obtained only slightly [26,27] but break down in most of the parameter space.

This model (11) can be easily incorporated into our theoretical framework. The result of the generating functional analysis (7) for this process (with or without thermal noise) can be obtained by replacing the average $\langle \cdots \rangle_\alpha$ by $\langle \cdots \rangle_\xi$ and the probability function $P_\alpha(S(t + 1)|S_1(t), \ldots, S_k(t))$ by

$$P_\xi(S(t + 1)|S(t); S_1(t), \ldots, S_k(t)) = \frac{e^{\beta S(t+1)\{\mathrm{sgn}[h(t)-2h]+S(t)\delta[h(t);2h]\}}}{2\cosh\beta\{\mathrm{sgn}[h(t) - 2h] + S(t)\delta[h(t); 2h]\}}, \quad (12)$$

where $h(t) = \sum_{j=1}^k \xi_j(1 + S_j(t))$.

In the case of $h \in \mathbb{R}$, the probability function (12) is independent of $S(t)$ and Eqs. (8)–(10) have the same structure for model (11): the α averages $\langle \alpha(S) \rangle_\alpha$ and $\langle \alpha(S)\alpha(\hat{S}) \rangle_\alpha$ are replaced by the averages

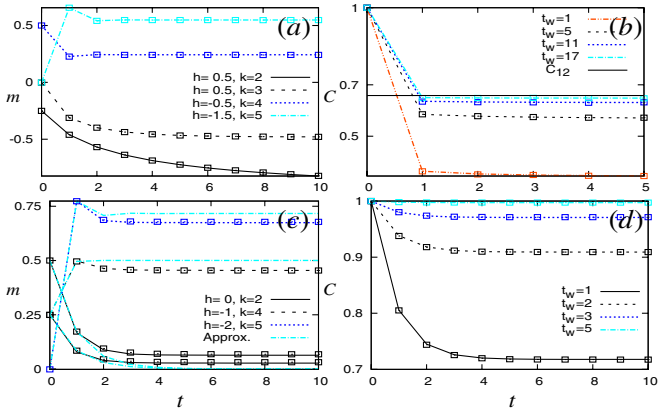

FIG. 1 (color online). Evolution of the magnetization [$m \equiv m(t)$] and correlation [$C \equiv C(t + t_w, t_w)$] functions with time t is governed by noiseless dynamics (11). Theoretical results (lines) are plotted against the results of MC simulations (symbols) with $N = 10^5$. Each MC data point is averaged over 10 runs. Error bars are smaller than symbol size. Top: Evolution of m (a) and C (b) for $h \in \mathbb{R}$. In (b) we plot C for $h = 0.5$ and $k = 3$. Bottom: Evolution of m (c) and C (d) for $h \in \mathbb{Z}$. In (d) we plot C for $h = 0$ and $k = 2$.

$\langle \mathrm{sgn}[h(t) - 2h] \rangle_\xi$ and $\langle \mathrm{sgn}[h(t) - 2h]\,\mathrm{sgn}[\hat{h}(t) - 2h] \rangle_\xi$, respectively. The equation for $m(t)$ recovers the annealed approximation result [12] [using the relation $b(t) = (1 + m(t))/2$]. In Figs. 1(a) and 1(b), we plot our analytical predictions for the evolution of $m(t)$ and $C(t + t_w, t_w)$ against the results of Monte Carlo (MC) simulation which use (11). The correlation function $C(t + t_w, t_w)$, in the limit of $t \to \infty$, $t_w \to \infty$, approaches the stationary solution of the overlap function (10) as predicted [Fig. 1(b)].

The situation is very different when $h \in \mathbb{Z}$. Then the magnetization $m(t) = \sum_{\boldsymbol{S}} P(\boldsymbol{S}) S(t)$, where $P(\boldsymbol{S})$ is a marginal of (7) with $P_\alpha \to P_\xi$, is no longer closed as in (8), but depends on $2^{t-1} - 1$ macroscopic observables (all magnetizations, all multitime correlations). Thus the number of macroscopic observables that determine the value of $m(t)$, or any other function computed from (7), grows exponentially with time. Annealed approximation results [12] for this model when $h \in \mathbb{Z}$ are only exact up to $t < 2$ time steps [the equation for $b(1) = (1 + m(1))/2$ in our approach and in [12] are identical] and deviate significantly from the exact solution at later times [Fig. 1(c)]. A typical evolution of the correlation function $C(t + t_w, t_w)$ in the system (11) when $h \in \mathbb{Z}$ is shown in Fig. 1(d).

BN are increasingly used for modeling of biological, social, and other physical systems. The theoretical framework developed here provides a systematic method for validating results obtained via the annealed approximation as well as a rigorous and powerful tool for future work in this area that copes with variability in Boolean functions, emerging correlations and memory effects.

Support by the Leverhulme trust (Grant No. F/00 250/H) is acknowledged.

[1] S. A. Kauffman, J. Theor. Biol. **22**, 437 (1969).
[2] S. Kauffman, *The Origins of Order* (Oxford University Press, New York, 1993).
[3] M. Aldana, S. Coppersmith, and L. P. Kadanoff, *Perspectives and Problems in Nonlinear Science.* (Springer, New York, 2003), pp. 23–89.
[4] B. Drossel, in *Reviews of Nonlinear Dynamics and Complexity* (Wiley, Weinheim, 2008), Vol. 1, Chap. 3, pp. 69–96.
[5] S. Kauffman, Nature (London) **224**, 177 (1969).
[6] B. Derrida, E. Gardner, and A. Zippelius, Europhys. Lett. **4**, 167 (1987).
[7] A. A. Moreira, A. Mathur, D. Diermeier, and L. A. N. Amaral, Proc. Natl. Acad. Sci. U.S.A. **101**, 12 085 (2004).
[8] B. Derrida and Y. Pomeau, Europhys. Lett. **1**, 45 (1986).
[9] B. Derrida and G. Weisbuch, J. Phys. (Paris) **47**, 1297 (1986).
[10] H. J. Hilhorst and M. Nijmeijer, J. Phys. (Paris) **48**, 185 (1987).
[11] J. Kesseli, P. Rämö, and O. Yli-Harja, Phys. Rev. E **74**, 046104 (2006).
[12] A. Szejka, T. Mihaljev, and B. Drossel, New J. Phys. **10**, 063009 (2008).
[13] C. De Dominicis, Phys. Rev. B **18**, 4913 (1978).
[14] M. Mezard, G. Parisi, and M. A. Virasoro, *Spin Glass Theory and Beyond* (World Scientific, Singapore, 1987).
[15] T. P. Peixoto and B. Drossel, Phys. Rev. E **79**, 036108 (2009).
[16] B. Derrida and H. Flyvbjerg, J. Phys. A **20**, L1107 (1987).
[17] A. Mozeika and D. Saad (to be published).
[18] K. Mimura and A. C. C. Coolen, J. Phys. A **42**, 415001 (2009).
[19] R. Kree and A. Zippelius, Phys. Rev. A **36**, 4421 (1987).
[20] We use the convention $\mathrm{sgn}[0] = 0$ throughout this Letter.
[21] T. P. Peixoto, Phys. Rev. Lett. **104**, 048701 (2010).
[22] W. Evans and L. Schulman, IEEE Trans. Inf. Theory **49**, 3094 (2003).
[23] S. N. Coppersmith, L. P. Kadanoff, and Z. Zhang, Physica (Amsterdam) **149D**, 11 (2001).
[24] J. A. de Sales, M. L. Martins, and D. A. Stariolo, Phys. Rev. E **55**, 3262 (1997).
[25] F. Li, T. Long, Y. Lu, Q. Ouyang, and C. Tang, Proc. Natl. Acad. Sci. U.S.A. **101**, 4781 (2004).
[26] R. Heckel, S. Schober, and M. Bossert, in *Proceedings of the 2010 International ITG Conference on Source and Channel Coding* (VDE Verlag, Berlin-Offenbach, 2010), pp. 1–6.
[27] J. G. T. Zañudo, M. Aldana, and G. Martínez-Mekler, arXiv:1011.3848.